JACC: CARDIOVASCULAR IMAGING VOL. 12, NO. 2, 2019

PUBLISHED BY ELSEVIER

FOCUS ISSUE: IMAGING IN AORTIC STENOSIS: PART II

ORIGINAL RESEARCH

Network Tomography for Understanding Phenotypic Presentations in Aortic Stenosis

Grace Casaclang-Verzosa, MD,[a,*] Sirish Shrestha, MSc,[a,*] Muhammad Jahanzeb Khalil, MD,[a] Jung Sun Cho, MD,[a] Márton Tokodi, MD,[a] Sudarshan Balla, MD,[a] Mohamad Alkhouli, MD,[a] Vinay Badhwar, MD,[b] Jagat Narula, MD, PhD,[c] Jordan D. Miller, PhD,[d] Partho P. Sengupta, MD, DM[a]

ABSTRACT

OBJECTIVES This study sought to build a patient–patient similarity network using multiple features of left ventricular (LV) structure and function in patients with aortic stenosis (AS). The study further validated the observations in an experimental murine model of AS.

BACKGROUND The LV response in AS is variable and results in heterogeneous phenotypic presentations.

METHODS The patient similarity network was developed using topological data analysis (TDA) from cross-sectional echocardiographic data collected from 246 patients with AS. Multivariate features of AS were represented on the map, and the network topology was compared with that of a murine AS model by imaging 155 animals at 3, 6, 9, or 12 months of age.

RESULTS The topological map formed a loop in which patients with mild and severe AS were aggregated on the right and left sides, respectively ($p < 0.001$). These 2 regions were linked through moderate AS; with upper arm of the loop showing patients with predominantly reduced ejection fractions (EFs), and the lower arm showing patients with preserved EFs ($p < 0.001$). The region of severe AS showed >3 times the increased risk of balloon valvuloplasty, and transcatheter or surgical aortic valve replacement (hazard ratio: 3.88; $p < 0.001$) compared with the remaining patients in the map. Following aortic valve replacement, patients recovered and moved toward the zone of mild and moderate AS. Topological data analysis in mice showed a similar distribution, with 1 side of the loop corresponding to higher peak aortic velocities than the opposite side ($p < 0.0001$). The validity of the cross-sectional data that revealed a path of AS progression was confirmed by comparing the locations occupied by 2 groups of mice that were serially imaged. LV systolic and diastolic dysfunction were frequently identified even during moderate AS in both humans and mice.

CONCLUSIONS Multifeature assessments of patient similarity by machine-learning processes may allow precise phenotypic recognition of the pattern of LV responses during the progression of AS. (J Am Coll Cardiol Img 2019;12:236–48) © 2019 by the American College of Cardiology Foundation.

From the [a]Division of Cardiology, West Virginia University Heart & Vascular Institute, Morgantown, West Virginia; [b]Department of Cardiovascular & Thoracic Surgery, West Virginia University Heart & Vascular Institute, Morgantown, West Virginia; [c]Division of Cardiology, Icahn School of Medicine at Mount Sinai, New York, New York; and the [d]Departments of Surgery, Cardiovascular Surgery, Physiology, and Biomedical Engineering, Mayo Clinic, Rochester, Minnesota. *Dr. Casaclang-Verzosa and Mr. Shrestha contributed equally to this work and are joint first authors. Dr. Sengupta has been a consultant for Heartsciences, Hitachi Aloka Ltd., and Ultromics. All other authors have reported that they have no relationships relevant to the contents of this paper to disclose. Dr. Blase A. Carabello served as Guest Editor for this paper.

Manuscript received August 16, 2018; revised manuscript received November 15, 2018, accepted November 28, 2018.

ISSN 1936-878X/$36.00 https://doi.org/10.1016/j.jcmg.2018.11.025

Aortic stenosis (AS) is the most common valvular lesion, with >1 in 8 individuals aged 75 years and older having moderate or severe AS (1). The disease starts as focal leaflet thickening with calcification and gradually progresses to obstruction of the left ventricular (LV) outflow tract (2). The LV response to AS is associated with LV hypertrophy, subendocardial ischemia, altered myocardial energetics, and fibrosis, which produce varying degrees of LV diastolic and systolic dysfunction (2,3). However, the LV response to AS is variable and is only partly determined by transaortic resistance (2,4,5). Although there is consensus in the cardiology community that phenotypic differentiation of types and stages of AS in association with the biology of the LV is essential for optimum risk stratification and clinical decision-making, strategies to achieve this important goal remain imprecise (5).

Advances in the field of genomics and systems biology have allowed the development of computational techniques that can identify complex relationships in data. Specifically, network biology is a powerful model for interpreting and contextualizing large diverse sets of biological data, for elucidating underlying complex biological processes, and creating an understandable model of a complex disease profile (6–8). We sought to use network analysis as an analytical method in which patients with varying stages of AS were represented in a multidimensional space. Using cross-sectional data, a compressed disease map was generated for exploration of possible paths that diseases such as AS can take as valvular dysfunction worsens in patients. We first used cross-sectional echocardiography data from a human population with varying AS severity to develop the disease map. Subsequently, we applied the same network analysis to an experimental murine model of progressive AS to determine whether this model effectively recaptured the phenotypic complexity of the human disease condition, and whether it could be used to guide further investigation into the clinically relevant ventricular and valvular phenotypes that emerge throughout the complex evolution of AS.

SEE PAGE 249

METHODS

PATIENT–PATIENT SIMILARITY NETWORK. Topological data analysis (TDA) uses a machine-learning framework to cluster patients and network visualization to derive novel insights into disease mechanisms. The network, or simplicial complex, that materializes from the compressed representation defines the shape of high-dimensional data (9–13). The fundamental shape of the data space is referred to as a "Reeb graph" in which nodes represent groups of patients who are similar to each other across multiple clinical features, whereas edges connect nodes that contain similar patients. The end result of

ABBREVIATIONS AND ACRONYMS

AS = aortic stenosis

AVA = aortic valve area

AVR = aortic valve replacement

EF = ejection fraction

LFLEF = low flow, low-gradient, low ejection fraction

LFpEF = low flow, low-gradient, preserved ejection fraction

LV = left ventricle

MACCE = major adverse cardiac and cerebrovascular event

NFLEF = normal flow, low ejection fraction

NFpEF = normal flow, preserved ejection fraction

RWT = relative wall thickness

TDA = topological data analysis

FIGURE 1 Steps of Topological Data Analysis

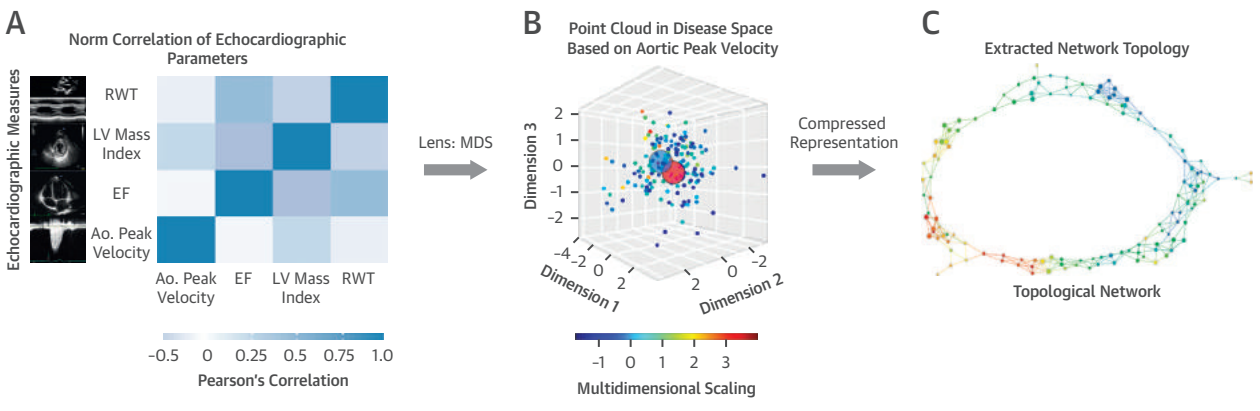

(A) Normalized bivariate correlation matrix of the 4 echocardiographic parameters of the dataset. **(B)** Data were processed using multidimensional scaling (MDS), and the first and second coordinates were applied as lenses to generate the disease space. The data points are colored according to the aortic peak velocity, which may be resampled several times by topological data analysis (TDA) to cluster patients into nodes **(red and blue circles)** and connect overlapping patients with edges. **(C)** TDA provides the compressed representation using nodes and edges for expressive visualization and interpretation. Ao. = aortic; EF = ejection fraction; LV = left ventricular; RWT = relative wall thickness.

FIGURE 2 Illustration of TDA Network With Coloration of Echocardiographic Parameters

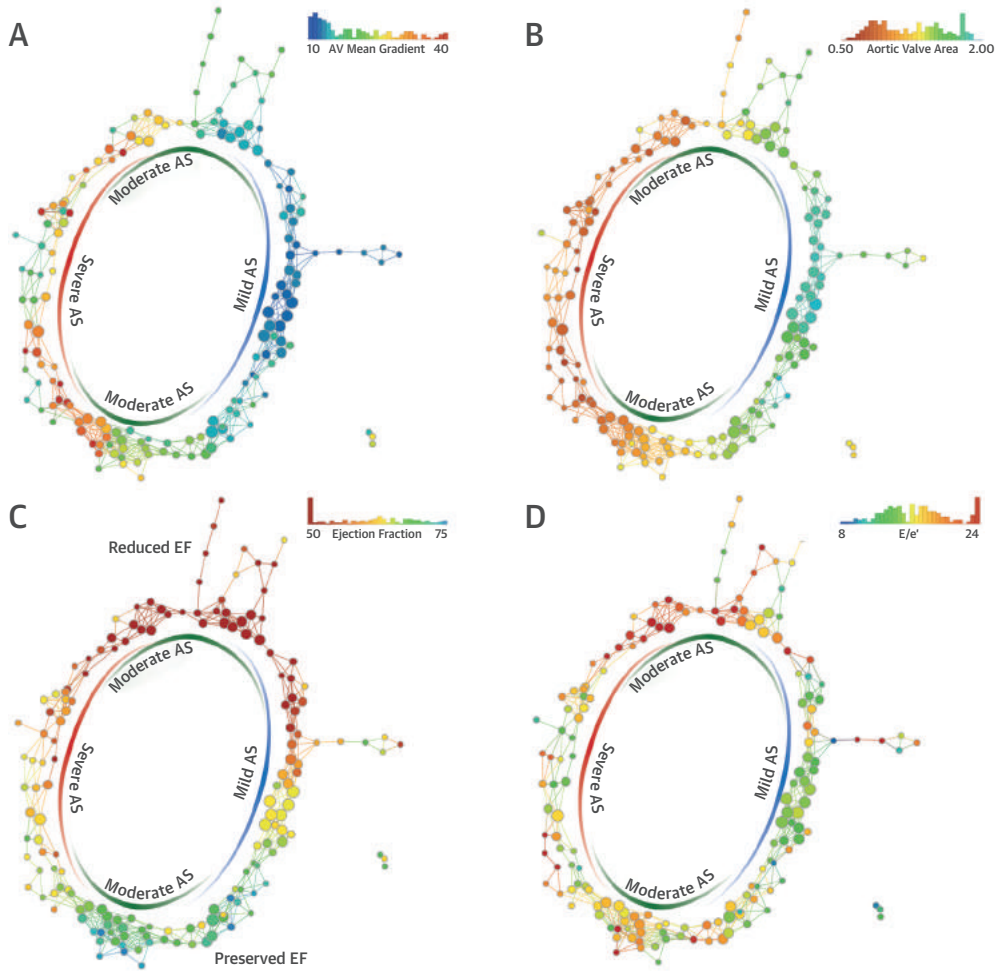

The similarity network draws aggregation of patients with severe and mild AS in 2 opposite ends and moderate AS in the top and bottom arms of the loop. The **red color** represents the abnormal values, whereas **blue** represents the normal or minor malady in the disease space. **(A)** Spectrum of mean gradient in humans identified in the network of disease space. High gradients aggregated on the **left side**, whereas the low gradients were on the **right side** with the moderate gradients in the **middle**. **(B)** Distribution of valve area on the network. **(C)** Patient similarity network revealing preserved and reduced ejection fractions (EFs) in the patients with aortic stenosis (AS). The top arm clustered patients with the reduced EF, whereas the bottom arm described the patients with preserved EF. The **red nodes** consist of patients with EFs of ≤50%, whereas the **blue nodes** consist of patient with EFs of ≥65%. **(D)** Distribution of E/e′ as a feature of diastolic dysfunction revealing the pattern of higher E/e′ around moderate and severe AS. The units of the **color bars on the top right of each panel** are the same as in Table 1. TDA = topological data analysis.

this process is a 2-dimensional chart that shows a level of similarity among various patient groups, all relative to one another. Two types of parameters are required to generate topological models: a metric that measures the similarity between data points; and lenses that are the functions that describe the distribution of the data and create overlapping bins of the dataset. Multiple lenses can be applied in the same analysis. Each lens has 2 tuning parameters: resolution and gain. Resolution determines the number of bins, whereas gain controls the overlapping between bins. The gain is adjusted so that most data points appear in a comparable number of bins. Equalizing the network distributes the patients evenly across all nodes in the network (9). TDA has been extensively validated and successfully applied in different areas of health sciences, such as gene expression profiling of breast tumors, identifying subgroups of type 2 diabetes, exploring endotypes of asthma, visualizing the syndromic space following central nervous system injury, and

TABLE 1 Comparison of the Topological Regions Predominantly* Containing Patients With Mild, Moderate, and Severe AS

	Region of Mild AS	Region of Moderate AS	Region of Severe AS	p Value
Age (yrs)	68 ± 15†	72 ± 14	78 ± 12‡	<0.001
Male	44 (53.66)	83 (50.00)	49 (49.49)	0.828
Coronary artery disease	32 (39.02)	66 (39.76)	41 (41.41)	0.942
Chronic renal failure	12 (14.63)	25 (15.06)	16 (16.16)	0.955
Hyperlipidemia	34 (41.46)	75 (45.18)	41 (41.41)	0.781
Diabetes mellitus	26 (31.71)	51 (30.72)	24 (24.24)	0.446
Hypertension	48 (58.54)	92 (55.42)	56 (56.57)	0.897
Cerebrovascular accident	10 (12.20)	29 (17.47)	18 (18.18)	0.491
LV end-diastolic diameter (cm)	4.73 ± 0.73	4.65 ± 0.83§	4.5 ± 0.61§	0.075
LV posterior wall, diastole (cm)	1.01 ± 0.2	1.09 ± 0.26	1.13 ± 0.27	0.012
LV mass index (g/m^2)	89.08 ± 35.11†	101.36 ± 38.25	106.85 ± 33.87‡	<0.001
Relative wall thickness	0.45 ± 0.12‡	0.5 ± 0.19	0.54 ± 0.17‡	<0.001
Types of remodeling pattern				0.017
Concentric remodeling	32 (39.02)	61 (36.75)	39 (39.39)	
Eccentric hypertrophy	7 (8.54)	15 (9.04)	7 (7.07)	
Concentric hypertrophy	12 (14.63)	46 (27.71)	36 (36.36)	
Ejection fraction <50%	10 (12.20)	36 (21.69)†	16 (16.16)	0.162
Doppler stroke volume index <35 ml/m^2	35 (42.68)§	93 (56.02)	76 (76.77)‡	<0.001
E/A ratio	1.36 ± 0.76	1.31 ± 0.81	1.22 ± 0.83	0.397
Septal e′ (cm/s)	6.73 ± 2.4§	6.15 ± 2.23	5.74 ± 1.93	0.014
Average E/e′	15.33 ± 8.02§	17.54 ± 9.27	18.18 ± 9.05	0.053
Left atrial volume index (ml/m^2)	37.6 ± 15.11	39.67 ± 17.82	41.67 ± 17.57§	0.228
TR peak gradient (mm Hg)	28.66 ± 9.62	30.87 ± 13.11	31.23 ± 14.23	0.449
Aortic valve area (cm^2)	1.69 ± 0.25‡	1.22 ± 0.34‡	0.84 ± 0.22‡	<0.001
Mean gradient (mm Hg)	11.81 ± 4.11‡	18.69 ± 10.67	27.67 ± 14.84‡	<0.001
Peak velocity (m/s)	2.34 ± 0.31‡	2.8 ± 0.66	3.33 ± 0.81‡	<0.001
Peak gradient (mm Hg)	22.21 ± 6.26‡	33.19 ± 16.59	47.11 ± 22.58‡	<0.001

Values are mean ± SD or n (%). *Nodes containing patients >50% with specific types of AS from sample for defining the regions. †$p < 0.01$. ‡$p < 0.001$. §$p < 0.05$ between the severe AS type and the remaining types.

AS = aortic stenosis; LV = left ventricular; TR = tricuspid regurgitation.

describing dynamics of malaria infections in humans and mice (6-8,10-13).

TDA of human cohort. TDA was performed using a cloud-based analytic platform (version 7.9, Ayasdi, Inc., Menlo Park, California). Seventy-nine separate clinical and echocardiographic variables were included as features. The initial TDA model was built using the following 4 echocardiographic variables: aortic valve area (AVA), LV ejection fraction (EF), LV mass index, and relative wall thickness (RWT) (**Figure 1**). We used a normalized correlation metric that measures the similarity between 2 points using Pearson's correlation on a normalized dataset, combined with 2 multidimensional scaling lenses (resolution: 24, gain: 2.5, equalized).

TDA of mice cohort. The TDA network was created using 4 echocardiographic parameters, namely, aortic peak velocity, EF, LV mass index, and RWT. Similar to the TDA network of the human cohort, the network of the mice was created with 2 lenses: metric principal component analysis coordinate 1 (resolution: 27, gain: 2.80, equalized) and metric principal component analysis coordinate 2 (resolution: 38, gain: 3.0, equalized).

STUDY POPULATION.

Human cohort. We included 246 patients (age 72 ± 14 years; 50% men) with AS who underwent echocardiographic evaluation at the Division of Cardiology, Heart and Vascular Institute, (Morgantown, West Virginia) from August 2017 to June 2018. Clinical features and risk factors were collected from patient medical records. AS severity was determined according to the recommendations of the European Association of Cardiovascular Imaging and the American Society of Echocardiography (14). Detailed methods for echocardiography assessment are presented in the Online Appendix. AS phenotypes were defined by the flow, mean gradient, and LV ejection fraction, as follows: normal flow, high-gradient, preserved EF (NFpEF) (SV ≥35 ml/m^2, EF ≥50%) low flow, low-gradient, low ejection fraction (LFLEF) (stroke volume index <35 ml/m^2; EF <50%); and low flow, low-gradient, preserved ejection fraction (LFpEF) (stroke volume index <35 ml/m^2; EF ≥50%).

FIGURE 3 Features of LV Hypertrophy Displayed on TDA

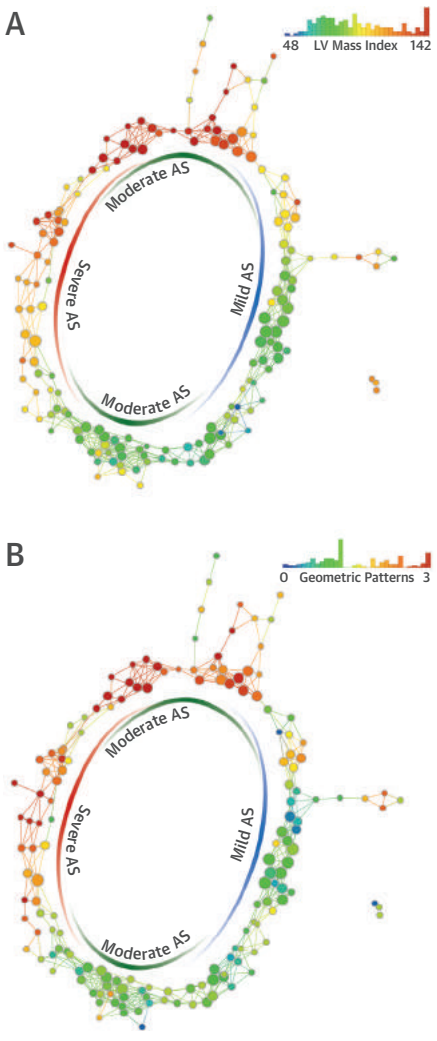

(A) Patients with reduced EF and severe AS show a higher LV mass index in the network. **(B)** TDA demonstrating the geometric patterns in the LV, in which the predominant patients with reduced EFs show eccentric and concentric hypertrophy. 0 = normal, 1 = concentric remodeling, 2 = eccentric hypertrophy, and 3 = concentric hypertrophy. Abbreviations as in Figures 1 and 2.

Patient electronic medical records were reviewed for post-echocardiographic follow-up. Endpoints were defined as surgical or transcatheter aortic valve replacement (AVR), hospitalization and/or death from major adverse cardiac and cerebrovascular events (MACCEs) (defined as myocardial infarction, acute coronary syndrome, acute decompensated heart failure, cardiac arrest, arrhythmia, stroke, or transient ischemic attack), and first MACCE hospitalization. The time to each endpoint was measured from index echocardiographic examinations. The West Virginia University Institutional Review Board approved all data collection and analysis.

Mouse cohort. Echocardiographic data for a murine model of AS (low-density lipoprotein receptor-deficient and/or apolipoprotein B100-only mice on a mixed c57BL/6J-129S7-129S4/SvJae-CBA/J background) were collected from an existing database at the Cardiovascular Disease and Aging Laboratory, Mayo Clinic (Rochester, Minnesota). Echocardiography measurements were performed at 3, 6, 9, and 12 months of age. A detailed description of the methods and protocols for comprehensive assessment of cardiac and valvular function in these mice was previously published and is presented in the Online Appendix (15). All methods and procedures were approved by the Mayo Clinic Institutional Animal Care and Use Committee.

Statistical analysis. Comparisons among multiple groups were performed using the Kruskal-Wallis test. Comparisons between a group of interest and the remaining subjects were performed using Pearson's chi-square test or Fisher's exact test (for categorical variables) and the nonparametric Kolmogorov-Smirnov test (for continuous variables). The rates of MACCE hospitalization and survival were analyzed using the Cox proportional hazard model. A p value of <0.05 was considered statistically significant. We used R (R Foundation, Vienna, Austria) and Python (Python Software Foundation, Beaverton, Oregon), including the Ayasdi software development kit, for all statistical analyses and TDA generation.

RESULTS

DISEASE MAP OF HUMAN AS. A topological network model was applied to cross-sectional clinical data from 246 consecutive patients with varying degrees of AS (Figures 2A to 2D). Differences in multivariate AS phenotypes were graded by location and color across the topological map. For our study, we referred to the different locations of the circular graph as the right side, middle, left side, top or upper arm, and bottom or lower arm. We also color-coded nodes red to indicate abnormal and/or severe, green and yellow to indicate intermediate, and blue to indicate normal and/or mild phenotypes. Table 1 shows the demographic and echo-Doppler distributions for patients grouped according to AVA. (For KS values, please refer to Online Table 1).

The network showed aggregation of blue nodes representing low AV mean gradients on the right side, green and yellow nodes with moderate gradients in the middle, and red nodes with high mean gradients on the left side (Figure 2A). This map coincided with the distribution of the AVA (Figure 2B). Overall, despite the clustering patterns, close examination revealed substantial overlap of nodes at the junction between mild and moderate AS and moderate and severe AS. We interpreted these data to mean that there was a significant multidimensional overlap in echocardiographic features across the 3 degrees of AS severity.

On examining the distribution of EFs, nodes that predominantly contained patients with reduced EFs (<50%) were found on the upper arm, whereas nodes with preserved EFs were situated on the lower arm (Figure 2C). The early diastolic transmitral flow velocity to mitral annular relaxation velocity ratio (E/e′) was higher in regions of moderate and severe AS (Figure 2D). The looped behavior of the network was preserved even after the addition of the E/e′ ratio as a marker of diastolic function (Online Figure 1).

Figure 3A and 3B shows the distributions of LV mass and the pattern of hypertrophy on the network. Patients with increased LV mass and concentric hypertrophy were predominantly found in the upper arm, extending to the left side toward severe AS.

We also examined whether there were differences between moderate AS in the upper and lower arms of the loop (Table 2; for KS values, please refer to Online Table 2). Patients with moderate AS in the upper arm had lower EFs ($p < 0.001$), were frequently men ($p = 0.013$), and a had higher incidence of coronary artery disease ($p = 0.003$). Although, patients in both arms had equal AVA ($p = 0.055$), patients in the upper area had a lower peak velocity ($p = 0.030$), a lower mean gradient ($p = 0.024$), a higher LV mass index ($p < 0.001$), and a higher left atrial volume ($p = 0.010$).

We further examined the topographic distribution of severe AS phenotypes within the disease map (Figure 4A to 4C). NFpEF severe AS phenotypes were located on 2 spots in the upper and lower left sides (Figure 4A), whereas the LFLEF phenotypes were clustered in the left upper side (Figure 4B) between NFpEF and LFLEF. LFpEF phenotypes aggregated on the left side (Figure 4C). Table 3 compares clinical and echocardiographic characteristics of the 3 severe AS phenotypes. (For KS values, refer to Online Table 3).

LONGITUDINAL FOLLOW-UP. During a follow-up of 157 days (range: 127 to 209 days), there were 33 MACCE hospitalizations, 4 cardiac deaths, and 35 surgical AVRs, transcatheter AVRs, or balloon valvuloplasties. MACCE hospitalization was equally distributed across all regions. However, there was >3 times the increased risk of transcatheter AVRs, surgical SAVRs, or balloon valvuloplasties (hazard ratio: 3.88; 95% confidence interval: 2.18 to 6.90; $p < 0.001$) among patients in the severe AS region compared with the remaining patients (Figure 4D). We analyzed follow-up echo-Doppler data of 35 patients who underwent AVR (Figure 5). After AVR, patients recovered their loci from the left side of the network (severe AS) to the middle and right side of the loop (moderate and mild AS).

TABLE 2 Comparison of the Topological Regions Predominantly* Containing Patients With Reduced and Preserved EF in Moderate AS

	Moderate: Reduced EF	Moderate: Preserved EF	p Value
Age (yrs)	76 ± 11	68 ± 14	0.421
Male	29 (63.04)	24 (39.34)	0.013
Coronary artery disease	25 (54.35)	16 (26.23)	0.003
Chronic renal failure	8 (17.39)	10 (16.39)	0.546
Hyperlipidemia	21 (45.65)	27 (44.26)	0.521
Diabetes mellitus	16 (34.78)	18 (29.51)	0.355
Hypertension	23 (50.00)	31 (50.82)	0.544
Cerebrovascular accident	8 (17.39)	9 (14.75)	0.456
End-diastolic diameter (cm)	5.25 ± 0.8	4.27 ± 0.58	<0.001
Posterior wall (cm)	1.12 ± 0.23	0.99 ± 0.15	0.005
LV mass index (g/m^2)	122.59 ± 40.67	73.67 ± 18.32	<0.001
Relative wall thickness	0.45 ± 0.14	0.47 ± 0.1	0.084
Types of remodeling pattern			<0.001
Concentric remodeling	7 (15.22)	40 (65.57)	
Eccentric hypertrophy	11 (23.91)	0 (0.00)	
Concentric hypertrophy	17 (36.96)	2 (3.28)	
Ejection fraction <50%	28 (60.87)	0 (0.00)	<0.001
Doppler stroke volume index (<35 ml/m^2)	25 (54.35)	28 (45.90)	0.252
E/A ratio	1.54 ± 1.0	1.08 ± 0.48	0.407
Septal e′ (cm/s)	5.25 ± 1.61	6.5 ± 2.08	0.003
Average E/e′	19.63 ± 9.3	16.73 ± 8.96	0.088
Left atrial volume index (ml/m^2)	47.46 ± 19.04	33.15 ± 13.04	0.010
TR peak gradient (mm Hg)	34.98 ± 15.15	30.66 ± 11.01	0.270
Aortic valve area (cm^2)	1.37 ± 0.33	1.22 ± 0.25	0.055
Mean gradient (mm Hg)	14.87 ± 6.49	20.39 ± 11.02	0.024
Peak velocity (m/s)	2.56 ± 0.52	2.89 ± 0.65	0.030
Peak gradient (mm Hg)	27.26 ± 11.93	35.3 ± 16.69	0.030

Values are mean ± SD or n (%). *Nodes containing patients >50% with specific types of AS from sample for defining the regions.

Abbreviations as in Table 1.

DISEASE MAP OF MURINE AS

The TDA map was generated from echo-Doppler data of 155 mice: 68 (38%) at 3 months old, 5 (2%) at 6 months old, 95 (53.3%) at 9 months old, and 10 (5%) at 12 months old using peak aortic velocity, LV mass index, LVEFs, and RWT in the model. A circular Reeb graph showed striking similarity to the Reeb graph

FIGURE 4 Patients With Phenotypes of Severe AS Represented on TDA

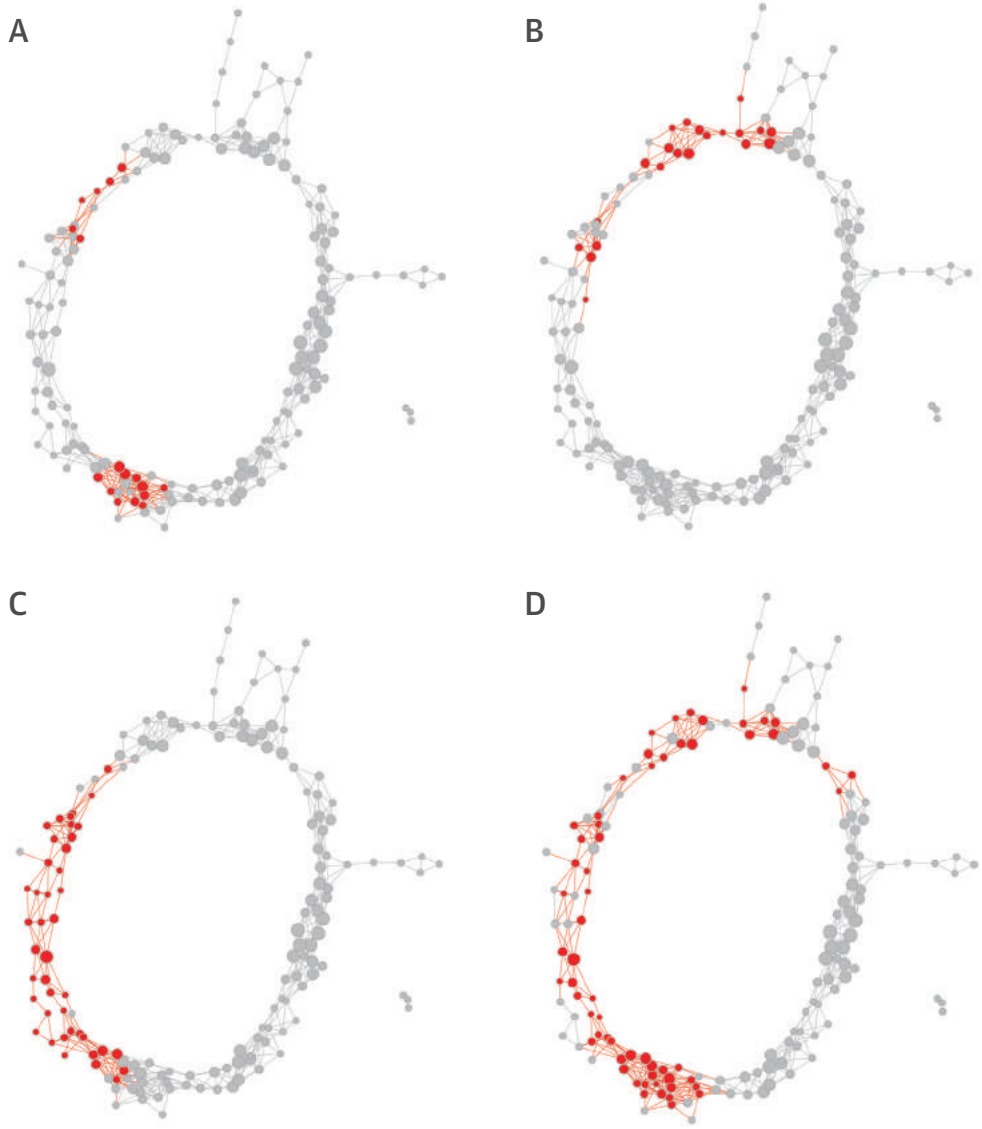

(A) Nodes containing severe AS patients with the normal flow, preserved EF phenotype (NFpEF). **(B)** Patients with low flow, low-gradient, low EF (LFLEF) severe AS phenotype aggregating on the nodes in the **left upper side** of the network. **(C)** Patients with low flow, low-gradient, preserved EF (LFpEF) are seen to span in nodes between NFpEF and LFLEF. **(D)** Nodes containing severe AS patients who received either transaortic valve replacement, surgical valve replacement, or balloon valvuloplasty. Abbreviations as in Figures 1 and 2.

derived from humans (Figure 6), including similar distributions of peak velocity, LV mass index, RWT, and LVEFs (Figures 6A to 6D).

For quantitative analysis, we grouped the mice into 3 groups based on the tertile of peak aortic velocity to describe the severity of AS (Table 4, for KS values, refer to Online Table 4). Mice in the lowest tertile (mild AS) showed larger cusp separation ($p < 0.01$), higher LVEFs ($p < 0.05$), RWT ($p < 0.001$), lower LV mass ($p < 0.01$), and lower E/e′ (39.9 ± 15.0; $p < 0.05$). Mice in the highest tertile (severe AS) had smaller cusp separation ($p < 0.05$), lower RWT ($p < 0.001$), higher LV end-diastolic dimension ($p < 0.01$), and higher E/e′ ($p < 0.05$). Topological locations were like those in humans, where mild AS was clustered on the right, moderate AS in the middle, and severe AS on the left side of the Reeb graph. Similar to human data, distinct

TABLE 3 Comparison of the Topological Regions Predominantly* Containing Patients With LFLEF, LFpEF, and NFpEF Severe AS Phenotypes

	LFLEF	LFpEF	NFpEF	p Value
Age (yrs)	78 ± 11†	77 ± 12†	75 ± 13	0.723
Male	27 (58.70)	38 (46.91)	17 (45.95)	0.378
Coronary artery disease	25 (54.35)‡	35 (43.21)	11 (29.73)	0.080
Chronic renal failure	9 (19.57)	15 (18.52)	6 (16.22)	0.923
Hyperlipidemia	16 (34.78)	33 (40.74)	19 (51.35)	0.308
Diabetes mellitus	13 (28.26)	19 (23.46)	10 (27.03)	0.816
Hypertension	24 (52.17)	45 (55.56)	23 (62.16)	0.654
Cerebrovascular accident	11 (23.91)	15 (18.52)	4 (10.81)	0.307
LV end-diastolic diameter (cm)	4.96 ± 0.64‡	4.36 ± 0.64†	4.51 ± 0.6	<0.001
LV posterior wall, diastole (cm)	1.22 ± 0.29§	1.12 ± 0.26	1.08 ± 0.24	0.029
LV mass index (g/m^2)	137.61 ± 40.77§	100.92 ± 27.55†	98.19 ± 38.73	<0.001
Relative wall thickness	0.52 ± 0.14‡	0.56 ± 0.2§	0.5 ± 0.13	0.391
Types of remodeling pattern				<0.001
Concentric remodeling	4 (8.70)	37 (45.68)	16 (43.24)	
Eccentric hypertrophy	6 (13.04)	5 (6.17)	2 (5.41)	
Concentric hypertrophy	29 (63.04)	25 (30.86)	9 (24.32)	
Ejection fraction <50%	26 (56.52)§	5 (6.17)†	4 (10.81)	<0.001
E/A ratio	1.5 ± 0.88	1.27 ± 0.98	1.17 ± 0.44	0.160
Septal e′ (cm/s)	5.31 ± 1.42†	5.73 ± 1.93	5.72 ± 1.8	0.566
Average E/e′	20.59 ± 10.36‡	17.76 ± 8.2	19.3 ± 9.18	0.369
Left atrial volume index (ml/m^2)	50.48 ± 18.97§	39.88 ± 16.01	38.49 ± 18.61	0.005
TR peak gradient (mm Hg)	32.86 ± 14.4	31.31 ± 14.23	28.35 ± 11.04	0.367
Aortic valve area (cm^2)	0.99 ± 0.36§	0.84 ± 0.21§	0.91 ± 0.23§	0.016
Mean gradient (mm Hg)	22.83 ± 13.1	27.18 ± 15.39§	30.0 ± 15.96§	0.082
Peak velocity (m/s)	3.02 ± 0.77	3.3 ± 0.84§	3.42 ± 0.85§	0.076
Peak gradient (mm Hg)	38.88 ± 19.87	46.62 ± 23.51§	49.74 ± 24.64§	0.065

Values are mean ± SD or n (%). *Nodes containing patients >50% with specific types of AS from sample for defining the regions. †$p < 0.01$. ‡$p < 0.05$. §$p < 0.001$ between the severe AS type and the remaining types.

LFLEF = low flow, low ejection fraction; LFpEF = low flow, preserved ejection fraction; NFpEF = normal flow, preserved ejection fraction; other abbreviations as in Table 1.

FIGURE 5 Patients in Network After AVR

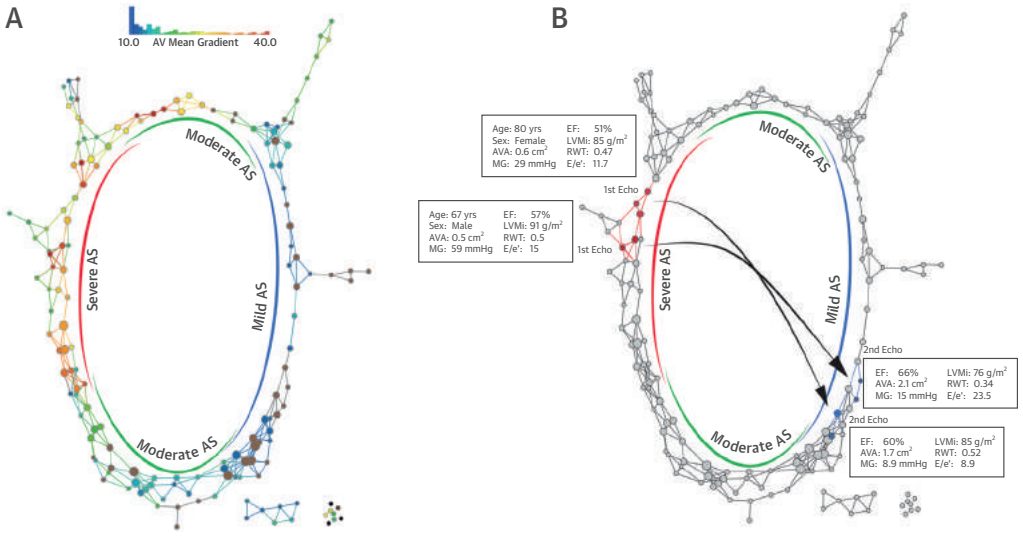

(A) Nodes containing patients imaged after aortic valve replacement (AVR) (**brown nodes**, median follow-up days: 36; range: 15 to 62 days) are depicted over the network and seen to aggregate in the region of mild or moderate AS. **(B)** Inter-region motion of 2 representative patients (64-year-old man and 80-year-old woman). AVA = aortic valve area; LVMi = left ventricular mass index; MG = mean gradient; other abbreviation as in Figures 1 and 2.

FIGURE 6 TDA From Echocardiography Performed in Mice Model of AS

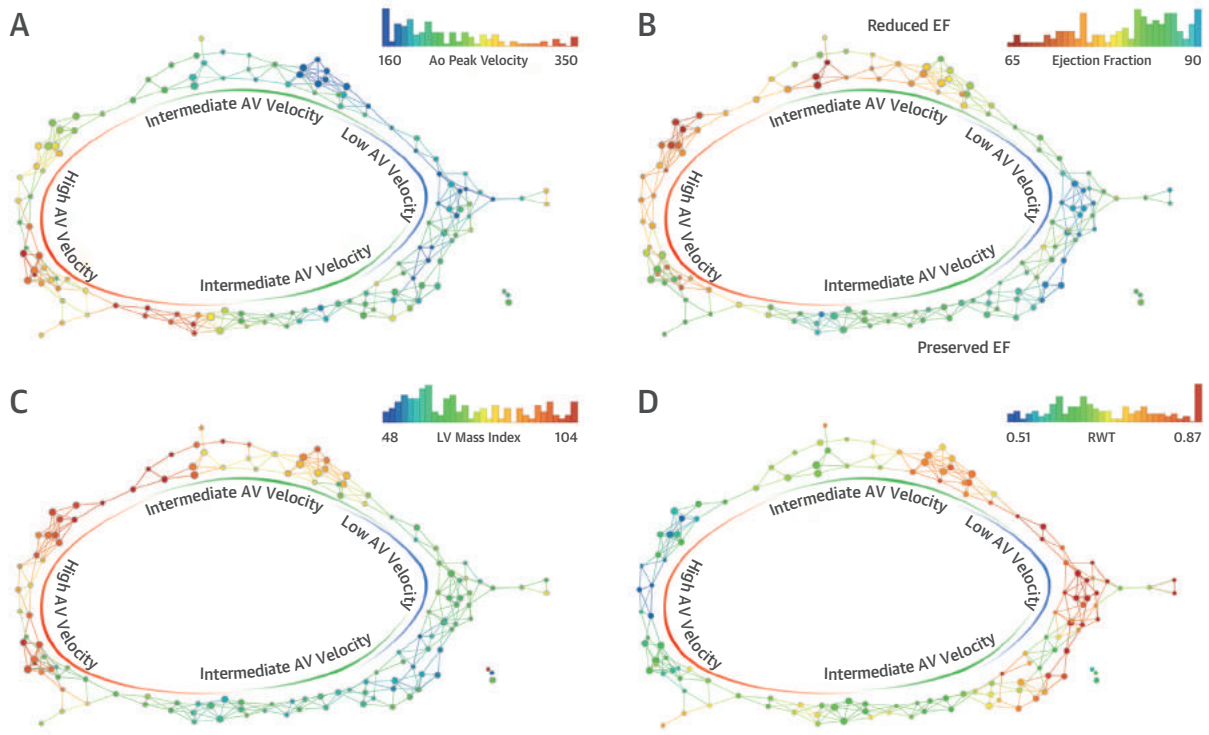

Map of the disease space in mice demonstrating the severity of AS as depicted by **(A)** aortic peak velocity, **(B)** EF, **(C)** LVMi, and **(D)** RWT. The color densities delineate exacerbation of the condition, where **red** signifies worse and **blue** signifies less severe AS. The **right side** of the disease map depicts mice in the first tertile (1.1 to 1.9 m/s), whereas the ones on the **left** are in high tertile (2.3 to 4.8 m/s) based on the peak velocity. Abbreviations as in Figures 1, 2, and 5.

differences were observed between the 2 arms of moderate AS. Mice in the upper arm had lower LVEFs ($p < 0.001$) and larger LV mass ($p < 0.001$) than mice in the lower arm (Table 5, for KS values, refer to Online Table 5).

LONGITUDINAL PROGRESSION OF AS IN MICE. To understand whether the topological map developed from cross-sectional mouse data was also indicative of the longitudinal progression of AS across their lifetime, we compared the nodes occupied by 2 groups of mice in which data with serial follow-up assessments were available for 3 and 6 months and for 3 and 9 months. By plotting longitudinal data from 7 mice assessed at 3- and 6-month time points, we observed a progressive right-to-left shift in the node locations on the loop space (Figure 7A). At 3 months, all 7 mice were located on the right side (lowest tertile) or in the upper (intermediate tertile) arm of the graph. At the 6-month follow-up, most of the mice had shifted from the right side to the left side, although a few remained in the lowest tertile zone. Similarly, we plotted longitudinal data from 7 mice assessed at 3- and 9-month time points, and we confirmed a similar progression (Figure 7B). At 3 months, the mice were distributed in 10 nodes on the right side of the loop (lowest tertile) and 8 nodes in the middle region (intermediate tertile). There were no mice located in the highest tertile region. However, at 9-month follow-up, a leftward shift in distribution was observed, with mice occupying 7 nodes on the left side (highest tertile of peak aortic velocity) and 4 nodes on the middle lower side of the loop (intermediate velocity zone). Six nodes on the right side of the loop remained occupied, which suggested that after 9 months, features of mild AS still existed. Collectively, these data suggested that the mouse model of AS was able to recapture the phenotypes of human AS using TDA.

DISCUSSION

AS is prevalent in 1.7% of the population age older than 65 years (1), and prospective natural progression

TABLE 4 Comparison of Predominantly* Low, Intermediate, and High Tertiles of AS Severity in Mice

	Predominantly Low	Predominantly Intermediate	Predominantly High	p Value
Age (months)	6 ± 3†	7 ± 3	7 ± 3	0.060
Male	30 (34.09)†	34 (34.34)†	39 (50.65)	0.045
Aortic peak velocity (m/s)	1.84 ± 0.44‡	2.02 ± 0.33‡	2.58 ± 0.68‡	<0.001
Cusp separation (mm)	0.89 ± 0.18§	0.86 ± 0.16	0.81 ± 0.16†	0.005
Heart rate (beats/min)	651.92 ± 83.99	656.03 ± 69.91	636.59 ± 80.98	0.071
Septum, diastole (mm)	0.98 ± 0.14	0.98 ± 0.15	0.95 ± 0.14	0.119
Septum, systole (mm)	1.62 ± 0.25	1.65 ± 0.25	1.62 ± 0.26	0.714
Isovolumic relaxation time (ms)	15.06 ± 6.02‡	13.78 ± 6.05	13.26 ± 6.83†	0.018
Isovolumic contraction time (ms)	7.73 ± 3.76§	7.15 ± 4.3	7.18 ± 5.77	0.278
End-diastolic diameter (mm)	2.63 ± 0.35‡	2.75 ± 0.42§	2.97 ± 0.47§	<0.001
End-systolic diameter (mm)	1.37 ± 0.38‡	1.43 ± 0.39†	1.59 ± 0.41	0.003
Posterior wall, diastole (mm)	0.97 ± 0.15	0.94 ± 0.13	0.93 ± 0.14	0.203
Posterior wall, systole (mm)	1.35 ± 0.21	1.34 ± 0.22	1.33 ± 0.25	0.777
LV mass (mg)	67.4 ± 19.73§	70.25 ± 22.38†	75.2 ± 20.78	0.034
Relative wall thickness	0.76 ± 0.14‡	0.72 ± 0.14	0.65 ± 0.14‡	<0.001
Ejection fraction (%)	81.77 ± 8.91†	81.13 ± 7.69	79.58 ± 7.93	0.167
Fractional shortening (%)	49.89 ± 9.21†	49.11 ± 8.5	47.53 ± 7.74	0.233
Pulmonary artery acceleration time (ms)	12.38 ± 3.29	11.73 ± 3.13	12.17 ± 6.01	0.271
Pulmonary artery ejection time (ms)	44.73 ± 7.05	43.62 ± 5.62	44.23 ± 6.64	0.274
LV outflow ejection time (ms)	39.2 ± 8.15	38.98 ± 6.1	38.88 ± 6.84	0.929
Average E/e′	39.19 ± 15.09§	41.48 ± 16.59	46.47 ± 19.53†	0.026
Septal e′ (mm/s)	23.96 ± 6.63†	23.39 ± 6.96	22.27 ± 7.5	0.202
E deceleration time (ms)	19.14 ± 6.44§	20.49 ± 6.51	21.85 ± 7.48	0.161
LV end-diastolic volume (ml)	31.27 ± 11.32	31.9 ± 12	33.84 ± 14.64	0.541
LV end-systolic volume (ml)	6.8 ± 4.89	7.22 ± 5.17	7.54 ± 6.03	0.659
Stroke volume index (ml/g BW)	1.03 ± 0.32	1.03 ± 0.35	1.05 ± 0.36	0.937

Values are mean ± SD or n (%). Aortic peak velocity is ordered and divided into 3 equal parts denoted as the low (109.1 to 184.5 cm/s), intermediate (185.2 to 234.3 cm/s), and high tertiles (234.5 to 475.5 cm/s). *Nodes containing mice >50% with specific types of AS from sample for defining the regions. †$p < 0.05$. ‡$p < 0.001$. §$p < 0.01$ between the severe AS type and the remaining types.

BW = body weight; other abbreviations as in Table 1.

studies are sparse, with the number of patients ranging from 100 to 400 (16,17). As with most age-associated diseases, a major challenge in studying the natural progression of AS is that its progression can span decades. For the first time, we described an alternative solution to provide a detailed characterization of the natural progression and subtypes of AS from cross-sectional data using TDA and demonstrated that a mouse model of AS was likely to recapture and parallel several key characteristics of the natural progression of AS in humans. The following sections highlight the implications and potential usefulness of these findings for the fields of both clinical and discovery science.

TDA AND PHENOTYPING AS. AS is a complex and heterogeneous disease with a phenotypic variation in disease progression and a LV response to increased afterload. Aortic valve calcification and stenosis progress at various rates in different patient populations, and the LV response to progressive overload is highly heterogeneous, even within well-defined patient subgroups with AS. Such variability makes this population highly susceptible to the generation of "high dimensional data." Newer scientific methods like TDA can therefore be useful for extracting meaningful knowledge through direct visualization of the heterogeneous datasets to enhance the potential of improved understanding and treatment of complex disorders like AS (9,13,18).

Although clinical stratification of patients at the extreme ends of disease can readily be accomplished with current clinical data (e.g., patients with mild or severe AS with negligible or severe ventricular dysfunction), our model suggested that it might be possible to identify a subset of patients who will experience aggressive deterioration of LV function at a much earlier time point. More specifically, a major important and novel observation in this study was the use of cross-sectional data for identification of 2 connected pathways through which mild forms of AS could progress to clinically severe forms of AS.

TABLE 5 Comparison of Upper and Lower Topological Regions in Intermediate AS in Mice

	Upper Arm	Lower Arm	p Value
Age (months)	7 ± 3	6 ± 3	0.281
Male	32 (48.48)	13 (32.5)	0.054
Aortic peak velocity (m/s)	2.01 ± 0.47	2.11 ± 0.45	0.327
Cusp separation (mm)	0.88 ± 0.16	0.89 ± 0.16	0.890
Heart rate (beats/min)	645.2 ± 71.57	644.55 ± 95.62	0.450
Septum, diastole (mm)	1.03 ± 0.12	0.9 ± 0.12	<0.001
Septum, systole (mm)	1.7 ± 0.26	1.54 ± 0.23	0.052
Isovolumic relaxation time (ms)	13.21 ± 5.71	15.13 ± 5.42	0.220
Isovolumic contraction time (ms)	6.72 ± 3.88	7.94 ± 3.69	0.304
End-diastolic diameter (mm)	3.09 ± 0.37	2.58 ± 0.23	<0.001
End-systolic diameter (mm)	1.81 ± 0.34	1.22 ± 0.24	<0.001
Posterior wall, diastole (mm)	1.01 ± 0.14	0.87 ± 0.11	<0.001
Posterior wall, systole (mm)	1.31 ± 0.19	1.34 ± 0.19	0.123
LV mass (mg)	90.04 ± 19.53	55.37 ± 9.97	<0.001
Relative wall thickness	0.67 ± 0.11	0.69 ± 0.1	0.837
Ejection fraction (%)	73.7 ± 7.83	86.15 ± 4.33	<0.001
Fractional shortening (%)	41.9 ± 6.55	54.2 ± 6.11	<0.001
Pulmonary artery acceleration time (ms)	11.82 ± 3.03	11.23 ± 3.46	0.744
Pulmonary artery ejection time (ms)	45.46 ± 7.06	43.33 ± 5.67	0.528
LV outflow ejection time (ms)	40.11 ± 7.05	38.05 ± 7.04	0.118
Average E/e′	41.35 ± 16.14	37.65 ± 11.28	0.407
Septal e′ (mm/s)	23.08 ± 7.36	24.27 ± 6.38	0.155
E deceleration time (ms)	21.19 ± 6.6	17.01 ± 4.3	0.003
LV end-diastolic volume (ml)	34.19 ± 14.67	32.21 ± 12.44	0.957
LV end-systolic volume (ml)	7.71 ± 6.52	7.32 ± 5.61	0.933
Stroke volume index (ml/g BW)	1.11 ± 0.33	1.05 ± 0.39	0.728

Values are mean ± SD or n (%). Aortic peak velocity is ordered and divided into 3 equal parts denoted as the low (109.1 to 184.5 cm/s), intermediate (185.2 to 234.3 cm/s), and high tertiles (234.5 to 475.5 cm/s).
Abbreviations as in Tables 1 and 4.

Notably, one pathway depicted the progression of valvular dysfunction with the preservation of EFs, and the second one suggested an accelerated decline in EFs despite disproportionally lesser degrees of valvular stenosis. Importantly, our study suggested that patients with preserved EFs had lower LV mass than patients with lower EFs, which suggested the existence of fundamental differences in the molecular adaptation to progressive ventricular overload in these 2 groups. We showed that LV systolic and diastolic dysfunction could occur even at early stages of aortic valve disease. More specifically, when tracking changes in EFs across the 3 zones of the TDA loop, our model suggested that a reduction in EF was not simply a linear and proportional consequence of progressive AS. Reduced LVEFs were observed in a significant cluster of patients with moderate AS in our dataset. Our observation was consistent with the findings of the study by Ito et al. (19), who reported that in some patients, the LVEF declined when AVA reached 1.2 cm^2. Although their study reported that a LVEF of <60% in the presence of moderate AS predicted further deterioration of LVEF, our model suggested that TDA modeling might be able to more accurately stratify such patients at an earlier stage for more aggressive medical management. However, a substantial overlap existed in patients with moderate and severe AS for valvuloventricular function. Collectively, these observations supported the use of integrative strategies that incorporated changes in LV function and aortic valve function in continuum for assessments of aortic valve syndromes to better understand phenotypic presentations in AS.

MOUSE MODEL OF AS. The use of a well-described mouse model of AS (low-density lipoprotein receptor-deficient, apolipoprotein B100-only) fed a high-cholesterol, high-fat diet to induce AS helped illustrate the validity of the TDA method (20–22). One major advantage of studying AS in mice is that they are the only species, other than humans, that have been shown to develop hemodynamically important stenosis (20–22). Perhaps more importantly, the relatively short lifespan of the mouse made it an attractive model for the study of time and/or age-dependent diseases such as AS. Moreover, echocardiographic evaluation of severity of AS in mice was refined using a high resolution imaging system, similar to that used in the present study (15). The reverse translational approach used in the study allowed us to match the echocardiography data between mice and humans to develop 2 closely resembled networks. More specifically, as AS progressed, there was a phenotypic bifurcation of mice with higher LV mass and lower EFs in 1 group and mice with lower LV mass and preserved EFs in the other group. Furthermore, we observed a lower EF in a subset of mice that had yet to reach severe stages of AS. Finally, the longitudinal data showed a variable rate of progression from mild AS, a phenomenon that is also seen in clinical practice. When combined, our observations showed that integrated measures of disease progression were associated not only with changes in valve function but also with Doppler parameters of LV systolic and/or diastolic function. Both progression along the network (seen in the mouse model from milder to higher gradient zones) and recovery along the network (seen in the human model when a patient moved from severe AS to mild AS zones after AVR) helped substantiate that the network model developed from cross-sectional data was also able to capture the longitudinal disease course or recovery (8).

CLINICAL IMPLICATIONS OF PRECISION PHENOTYPING IN AS. The valvulo-ventricular complex is an integral part of the disease process from which patients' symptoms likely arise, but is not due to AS, per se. However, current guidelines rely on velocity and/or gradients, AVA, LVEF, and stroke volume to decide on phenotypic presentation and the timing of intervention (23). Our study provided patient similarity-based recognition of phenotypic presentations and suggested that different stages and grades of disease severity in AS occurred along a phenotypic continuum rather than in arbitrary divisions based on a few isolated measurements and thresholds. Accordingly, some patients with AVA that suggested severe AS showed phenotypic similarity to a lower severity of AS and vice versa. Interestingly, several patients with moderate AS developed LV dysfunction. Our data suggested that several of these patients had phenotypic similarity with severe AS, thereby making the case for early intervention. There is a need to develop precision phenotyping models using machine-learning algorithms so that surveillance and intervention can be tailored to individual patients. In the future, TDA-based analysis of longitudinal data might help clinicians visualize patients on a disease map and predict the natural disease progression based on how patients in a similar cluster progressed over time and how they responded to therapies.

STUDY LIMITATIONS. Our human and mouse datasets were limited in numbers, and all phenotypes might not have been well represented. Larger cohorts of patients and animal data sampled at multiple time points and assessment of clinical outcomes are needed to validate TDA as a viable methodology for predicting natural disease progression, guiding individual patient treatments, and assessing prognosis.

CONCLUSIONS

We demonstrated the use of TDA as a tool to study the natural progression of disease from cross-sectional and follow-up human data. Our model strongly suggested that both patients with AS and animal models of AS progressed via 1 of 2 predominant pathways as disease progressed from mild to severe stenosis, with 1 pathway preserving EFs and the other pathway characterized by deterioration of EFs. Collectively, our data and TDA model supported the use of integrated valvulo-ventricular stratification of subgroups with AS, which warrants future investigations in both clinical- and discovery-focused studies.

FIGURE 7 TDA for Assessing Longitudinal Disease Pathway in Mice

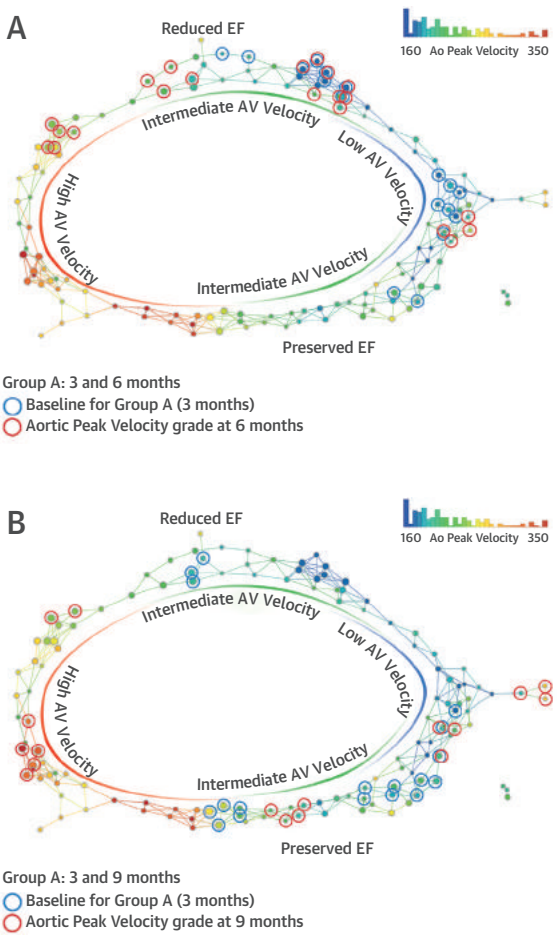

A topological network map comparison of the location of mice based upon peak AV velocity at **(A)** 3 and 6 months and **(B)** 3 and 9 months, respectively. The **blue circles** signify 3-month mice, whereas **red** signifies AV velocity grade at 6 and 9 months for **A and B**, respectively. Abbreviations as in Figures 1, 2, and 6.

ACKNOWLEDGMENTS The authors are grateful to Joel Dudley, Icahn School of Medicine at Mount Sinai and to Ayasdi, Inc. (Menlo Park, California), especially Devi Ramanan, for topological data analysis support and collaborative access.

ADDRESS FOR CORRESPONDENCE: Dr. Partho P. Sengupta, Heart and Vascular Institute, West Virginia University, 1 Medical Center Drive, Morgantown, West Virginia 26506-8059. E-mail: partho.sengupta@wvumedicine.org.

PERSPECTIVES

COMPETENCY IN MEDICAL KNOWLEDGE: Similar to expert clinician knowledge, TDA, without a priori knowledge, can merge multiple transthoracic echocardiographic measurements of AS severity, including LV wall thickness, cavity dimensions, stroke volume, and EFs to extract phenotypic presentations in AS. Furthermore, patients can be individually delineated for mapping disease progression or recovery.

TRANSLATIONAL OUTLOOK: Future clinical trials should merit using data-driven approaches like TDA for identifying and risk stratifying AS patient subgroups so that surveillance and interventions can be tailored to individual patients.

REFERENCES

1. Nkomo VT, Gardin JM, Skelton TN, Gottdiener JS, Scott CG, Enriquez-Sarano M. Burden of valvular heart diseases: a population-based study. Lancet 2006;368:1005–11.

2. Iung B, Vahanian A. Degenerative calcific aortic stenosis: a natural history. Heart 2012;98 Suppl 4: iv7–13.

3. Dweck MR, Boon NA, Newby DE. Calcific aortic stenosis: a disease of the valve and the myocardium. J Am Coll Cardiol 2012;60:1854–63.

4. Chambers J. The left ventricle in aortic stenosis: evidence for the use of ACE inhibitors. Heart 2006;92:420–3.

5. Carabello BA. What is severe aortic stenosis and why do people die from it? J Am Coll Cardiol Img 2016;9:806–8.

6. Torres BY, Oliveira JH, Thomas Tate A, Rath P, Cumnock K, Schneider DS. Tracking resilience to infections by mapping disease space. PLoS Biol 2016;14:e1002436.

7. Offroy M, Duponchel L. Topological data analysis: a promising big data exploration tool in biology, analytical chemistry and physical chemistry. Anal Chim Acta 2016;910:1–11.

8. Bruno JL, Romano D, Mazaika P, et al. Longitudinal identification of clinically distinct neurophenotypes in young children with fragile X syndrome. Proc Natl Acad Sci U S A 2017;114: 10767–72.

9. Lum PY, Singh G, Lehman A, et al. Extracting insights from the shape of complex data using topology. Sci Rep 2013;3:1236.

10. Nielson JL, Paquette J, Liu AW, et al. Topological data analysis for discovery in preclinical spinal cord injury and traumatic brain injury. Nat Commun 2015;6:8581.

11. Saggar M, Sporns O, Gonzalez-Castillo J, et al. Towards a new approach to reveal dynamical organization of the brain using topological data analysis. Nat Commun 2018;9:1399.

12. Nielson JL, Cooper SR, Yue JK, et al. Uncovering precision phenotype-biomarker associations in traumatic brain injury using topological data analysis. PLoS One 2017;12: e0169490.

13. Li L, Cheng WY, Glicksberg BS, et al. Identification of type 2 diabetes subgroups through topological analysis of patient similarity. Sci Transl Med 2015;7:311ra174.

14. Baumgartner H, Hung J, Bermejo J, et al. Recommendations on the echocardiographic assessment of aortic valve stenosis: a focused update from the European Association of Cardiovascular Imaging and the American Society of Echocardiography. J Am Soc Echocardiogr 2017; 30:372–92.

15. Casaclang-Verzosa G, Enriquez-Sarano M, Villaraga HR, Miller JD. Echocardiographic approaches and protocols for comprehensive phenotypic characterization of valvular heart disease in mice. J Vis Exp 2017;120:e54110.

16. Brener SJ, Duffy CI, Thomas JD, Stewart WJ. Progression of aortic stenosis in 394 patients: relation to changes in myocardial and mitral valve dysfunction. J Am Coll Cardiol 1995;25: 305–10.

17. Rosenhek R, Zilberszac R, Schemper M, et al. Natural history of very severe aortic stenosis. Circulation 2010;121:151–6.

18. Romano D, Nicolau M, Quintin EM, et al. Topological methods reveal high and low functioning neuro-phenotypes within fragile X syndrome. Hum Brain Mapp 2014;35:4904–15.

19. Ito S, Miranda WR, Nkomo VT, et al. Reduced left ventricular ejection fraction in patients with aortic stenosis. J Am Coll Cardiol 2018;71: 1313–21.

20. Drolet MC, Roussel E, Deshaies Y, Couet J, Arsenault M. A high fat/high carbohydrate diet induces aortic valve disease in C57BL/6J mice. J Am Coll Cardiol 2006;47:850–5.

21. Weiss RM, Ohashi M, Miller JD, Young SG, Heistad DD. Calcific aortic valve stenosis in old hypercholesterolemic mice. Circulation 2006;114: 2065–9.

22. Miller JD, Weiss RM, Heistad DD. Calcific aortic valve stenosis: methods, models, and mechanisms. Circ Res 2011;108:1392–412.

23. Nishimura RA, Otto CM, Bonow RO, et al. 2014 AHA/ACC Guideline for the management of patients with valvular heart disease: executive summary: a report of the American College of Cardiology/American Heart Association Task Force on Practice Guidelines. J Am Coll Cardiol 2014;63: 2438–88.

KEY WORDS aortic stenosis, left ventricular function, patient similarity, topological data analysis

APPENDIX For an expanded Methods section as well as supplemental figures and tables, please see the online version of this paper.